DETERMINATION OF THE TRANSFORMATION EXPONENT S FROM EXPERIMENTS AT CONSTANT HEATING RATE

M.J. Starink* and A.-M. Zahra

Centre de Thermodynamique et de Microcalorimétrie du CNRS,
13331 Marseille Cedex 3, France

*currently (since 1998): Materials Research Group, School of Engineering Sciences,
University of Southampton, Southampton S017 1BJ, UK
e-mail: m.j.starink@soton.ac.uk

Abstract

The transformation exponent s is characteristic for the mechanism of a reaction and contains information on nucleation rate and type of growth; it corresponds to the Avrami parameter n in isothermal experiments. Two methods for the determination of s from experiments performed at constant heating rate are presented. They consist of plotting either the logarithm of the reaction rate or of the amount transformed vs. 1/T, and s can subsequently be calculated from the slope of the initial straight line. The methods are successfully applied to precipitation in Al-6at%Si, GPB-zone formation in Al-Cu-Mg based alloys, and recrystallisation of deformed FCC metals.

Keywords: linear heating, Avrami parameter, transformation exponent, Johnson-Mehl-Avrami-Kolmogorov (JMAK) kinetics, GPB zone

1.   Introduction

Whilst isothermal experiments are generally very time consuming, experiments performed at constant heating rate (linear heating) are a much more rapid way of studying a transformation. Another disadvantage of isothermal analysis is the impossibility of reaching a test temperature instantaneously, and during the time which the system needs to stabilise no measurements are possible. Linear heating experiments do not have this drawback as, in principle, scanning can always be started at a temperature sufficiently low to avoid reaction in the first stages of the experiment. As a result of these advantages experimental methods involving temperature scanning, like Differential Scanning Calorimetry (DSC) or Thermogravimetry (TG), have gained in popularity. (It should, however, be mentioned that temperature scanning methods have their own particular drawbacks, like temperature inhomogeneities in the system or the in the sample.) For the analysis of these types of experiments it would be advantageous to obtain analysis methods based on the same principles as the Johnson-Mehl-Avrami-Kolmogorov (JMAK) equation (see e.g. Refs. [1,2,3]) for isothermal reactions. For instance, for a reaction which conforms to JMAK kinetics one can obtain the Avrami parameter, n, which characterises a reaction, from the slope of

1

a plot of $\ln[-\ln(1-\alpha)]$ vs. $\ln t$, where t is the time and α the fraction transformed (see e.g. Ref. [1]). This type of plot is often referred to as an Avrami plot.

In the past 10 years three methods to derive the Avrami parameter, n, for reactions occurring during linear heating have been proposed: the Woldt method [4,5], the Criado-Ortega method [6], and the Lee-Kim [7] method. The first two methods are based on JMAK kinetics, whilst the latter is an extension of the Criado-Ortega method and takes account of impingement which does not conform to the JMAK model. However, none of these methods has been used much beyond the papers in which they were introduced. This is suggested to be due to the following drawbacks of these methods. Firstly, whilst a large number of reactions do not correspond to JMAK kinetics, or correspond to JMAK kinetics only over a limited temperature range [2,8,9,10,11,12], the Woldt and the Criado-Ortega methods are only valid for reactions which correspond to JMAK kinetics. Secondly, the Woldt method is much more complicated than the isothermal method using the Avrami plot. Further, due to the use of Doyle's approximation for the temperature integral (see Ref. [6]), the Criado-Ortega and the Lee-Kim methods can give rise to inaccuracies. (Lee and Kim [7] indicated improved approximations for limited temperature ranges, but they come at the expense of further complications in the methods.) In addition it is noted that all three methods, like many works on the theory of the kinetics of phase transformations, assume the validity of the kinetic equation of the type:

$$\frac{d\alpha}{dt} = k(T)f(\alpha) \tag{1}$$

with $f(\alpha)$ a function depending only on the fraction transformed, and $k(T)$ a function of temperature. However, in various cases this expression is not valid [13,14]. From these drawbacks of the three methods it is concluded that a new simple, yet accurate method, with a more general validity, will be very useful.

Recently, Starink and Zahra [15] presented a model for the analysis of nucleation and growth type reactions at constant heating rate. A key element of the model is the assumption that, similar to the JMAK model, the transformed volume, V_p, around a single nucleus grows according to:

$$V_p = A[G(t-z)]^m \tag{2}$$

where G is the (average) growth rate, A is a constant, z is the time at which the nucleus is formed, whilst m is a constant related to the dimensionality of the growth and the mode of transformation. We will term m the growth exponent, generally it is a multiple of 0.5 for diffusion controlled growth and a multiple of 1 for a reaction with constant rate of movement of the interface (linear growth) (see e.g. Ref. [1]). It was shown that by assuming an Arrhenius type temperature dependency of both the growth rate and the nucleation rate, the fraction transformed during the initial stages, when impingement is negligible, increases with temperature, T, as:

$$\alpha_{ext} \cong \left(A_1 \exp\left[\frac{-E_{eff}}{k_B T}\right] T^2 \right)^s \tag{3}$$

where A_1 is a constant, E_{eff} is the effective activation energy, α_{ext} is the fraction transformed in the hypothetical case where no impingement occurs and k_B is Boltzman's constant. In this equation the exponent s is an important characteristic for the reaction and we will term it the transformation exponent; it is akin to the Avrami parameter in isothermal analysis.

By further considering impingement and the variation of the solvus with temperature a model describing the amount transformed as a function of temperature and heating rate was obtained (the model will be reviewed in Section 3.1), and fits of this model to DSC effects of precipitation in Al-Mg and Al-Si alloys showed a near perfect match [15]. As evaluation of the equations in this model requires some (limited) computing power, the derivation of values for the transformation exponent from these fits is somewhat cumbersome. For this reason we will in this paper present a simplified but still quite accurate procedure for obtaining the transformation exponent s from transformation curves directly, without the need to fit the whole of the curve.

The method is first verified, and subsequently applied to DSC curves of technologically important Al-based alloys. Firstly, we will study precipitation in an Al-6at%Si alloy. Due to their excellent castability, high silicon Al-Si alloys (Si content in excess of ~5at%) are technologically important, and the present study will enhance the understanding of heat treatment of these alloys. Secondly, we will study GPB-zone formation in Al-Cu-Mg based alloys. For this we have selected a ternary Al-Cu-Mg model alloy which forms the basis of the AA2000 series of alloys, an Al-Cu-Mg alloy with added grain refiner (Zr), and the 8090 (Al-Li-Cu-Mg-Zr) alloy, which is a relatively new, low density alloy for aerospace applications. In addition we will study recrystallisation in deformed FCC metals.

2.   Experimental

For the experiments conventionally cast, high purity Al-Si, Al-Cu-Mg and Al-Cu-Mg-Zr alloys, and a powder metallurgical, commercial purity Al-Li-Cu-Mg-Zr (8090) alloy were used. For details on alloys and sample preparation, see Refs. [15,16,17,18]. Compositions are given in Table 1. Machined samples were solution treated at 550°C for the Al-Si alloy, at 520°C for the 8090 alloy and at 525°C for the other two alloys. Solution treatment was generally terminated by quenching in water at room temperature. For the Al-Si alloy also cooling at 200°C/min in a DSC apparatus was performed.

For DSC experiments disks of 6 mm diameter and 1 mm thickness were used. DSC experiments were performed using a Perkin-Elmer 1020 series DSC7 (for the Al-Si alloy), a Shimadzu DSC-50 (for the 8090 alloy) and a DuPont model 990 DSC (for Al-Cu-Mg and Al-Cu-Mg-Zr). Details on calibration procedures, baseline correction and correction for heat capacity have been given elsewhere [15,17,18,19]. DSC curves presented reflect the heat flow due to reactions, negative heat flows reflect exothermic reactions.

Table 1   Composition of the alloys (in at %).

alloy	Cu	Mg	Li	Zr	Si	Al
Al-6Si	-	-	-	-	5.8	balance
Al-Cu-Mg	0.87	1.44	-	-	0.006	balance
Al-Cu-Mg-Zr	0.90	1.46	-	0.03	0.04	balance
Al-Cu-Mg-Li-Zr (8090)	0.50	1.09	8.6	0.03	~0.2	balance

In addition, isothermal calorimetry was employed. Batches of 20 disk shaped samples of 1 mm thickness were prepared and examined in a differential Tian-Calvet microcalorimeter which possesses an excellent base line stability coupled with a high sensitivity (down to a microwatt). The baseline of the microcalorimeter at each temperature was determined by performing experiments with pure Al. Further details of the experimental procedures are presented in Ref. 13.

3 Theory and analysis methods

3.1 Nucleation and growth reactions at constant heating rate

In this section a brief outline of the recently derived model for nucleation and growth reactions at constant heating rate will be given. For a more complete description and a discussion of the various elements of the model the reader is referred to Ref. 15.

For diffusion controlled precipitation reactions, we will define the transformed volume to be the volume of an imaginary fully depleted area around a precipitate (with the rest of the matrix undepleted) needed to give a precipitate size equal to the real case with a diffusion zone. For reactions without a diffusion zone the definition of the transformed volume is straightforward. In general, the volume, V_p, of the transformed region at time t is given by Eq. 2. If all transformed volumes grow without impinging (the so-called extended volume approach, see Refs. [1] and [3]), the total transformed volume is given by $V_{ext}(t)$. We introduce the variable $\alpha_{ext} = V_{ext}/V_o$, where V_o is the volume of the sample, and assume that both the growth rate and the nucleation rate can be described by Arrhenius type dependencies (see also Refs. [4,5,15]). To obtain α_{ext} a temperature integral needs to be evaluated. This integral can be approximated to yield:

$$\alpha_{ext} \cong \left(\frac{\beta k_B}{E_G} k_c \exp\left[\frac{-E_{eff}}{k_B T} \right] \left(\frac{T}{\beta} \right)^2 \right)^s \tag{4}$$

where

$$E_{eff} = \frac{m E_G + E_N}{m+1} \tag{5}$$

$$s = m + 1 \tag{6}$$

in which E_G and E_N are the activation energies for growth and nucleation, respectively, β is the heating rate, and k_c is a constant. The above approximation of the temperature integral has been shown to be highly accurate (see Ref. [4]) and it is certainly more accurate than Doyle's approximation of the temperature integral [20], which forms the basis of the Criado-Ortega [6] and the Lee-Kim [7] methods. Also for the case where nuclei are present before the start of the transformation and no further nucleation occurs, Eq. 4 is in good approximation valid. In this case $s = m$ and $E_{eff} = E_G$.

Impingement is taken account of by using:

$$\frac{d\alpha}{d\alpha_{ext}} = (1-\alpha)^{\lambda_i} \tag{7}$$

where λ_i will be termed the impingement factor (see also Ref. [8]). The general solution of Eq. 7 for $\lambda_i \neq 1$ is:

$$\alpha = 1 - \left(\frac{\alpha_{ext}}{\eta_i} + 1 \right)^{-\eta_i} \tag{8}$$

where $\eta_i = 1/(\lambda_i -1)$.

In some precipitation reactions several processes with different s can occur. When impingement of precipitates formed by dissimilar processes is negligible as compared to impingement between

precipitates formed by the same process, the processes essentially occur in independent volumes of the alloy, and one can obtain the sum of two processes simply from a weighted average:

$$\xi = f\,\xi_1 + (1-f)\,\xi_2 \tag{9}$$

where f is the volume fraction of the alloy in which process 1 occurs and (1-f) is the volume fraction of the alloy in which process 2 occurs, whilst ξ is the amount of atoms incorporated in the growing nuclei divided by the maximum amount of atoms that can be incorporated according to the equilibrium phase diagram.

To account for the variation of the equilibrium state with temperature we assume that the variation of the equilibrium or metastable equilibrium concentration, $c_{eq}(T)$, as a result of the increase in temperature is relatively slow as compared to variations in the local concentrations of alloying atoms due to diffusion of atoms. From this follows:

$$\dot{\xi} = \frac{d\xi}{dt} = \frac{d}{dt}\left[\alpha\,\frac{c_o - c_{eq}(T)}{c_o}\right]A_2 \tag{10}$$

where A_2 is a constant.

Application of Eq. 10 requires data on $c_{eq}(T)$. For Al-Si this data is readily available (see Ref. [21]), and $c_{eq}(T)$ can be described well by a regular solution model (see Refs. [15,22]).

3.2   Direct determination of the transformation exponent s

Throughout this section we consider the first stages of the reaction at which impingement is negligible. This stage should be situated well before $\dot{\xi}$ reaches its first inflection point. If we assume that for this narrow temperature range at the beginning of the reaction the variation of the equilibrium state with the temperature is negligible, we may approximate:

$$A_3\,\xi \cong \alpha_{ext} \cong \left(\frac{\beta k_B}{E_G}\,k_c\,\exp\left[\frac{-E_{eff}}{k_B T}\right]\left(\frac{T}{\beta}\right)^2\right)^s \tag{11}$$

where A_3 and subsequent A_4 to A_8 are constants. Taking the logarithm yields:

$$\ln \xi \cong \frac{-s E_{eff}}{k_B T} + 2\,s\,\ln T + A_4 \tag{12}$$

Hence if E_{eff} is known (see Section 3.3), s can be obtained from the slope of a plot of $\ln\xi$ vs. $2\ln T\text{-}E_{eff}/k_B T$. As the variation in s lnT is generally much smaller than the variation in $E_{eff}/k_B T$, one may further approximate by plotting $\ln\xi$ vs. $\text{-}E_{eff}/k_B T$ and obtain s from the slope by using:

$$k_B\,\frac{d\ln\xi}{d\,1/T} \cong -s\left(E_{eff} + 2k_B T_{av}\right) \tag{13}$$

where T_{av} stands for the average temperature of the (narrow) temperature range considered. It is further noted that as a result of taking the logarithm and the derivative we may, in Eq. 13, insert any variable proportional to ξ in place of ξ. For DSC this means that we can use the integrated evolved heat, $\Delta Q(T)$, instead of ξ.

5

For a derivative type thermal analysis method like DSC the signal is proportional to $\dot{\xi}$, and it would be advantageous to obtain the transformation exponent s directly from the DSC heat flow signal without having to perform the integration of the signal. To obtain such a method we will first calculate the rate of the reaction from Eq. 11:

$$\dot{\xi} \cong A_5 s \exp\left[\frac{-sE_{eff}}{k_B T}\right]\left(\frac{E_{eff}}{k_B} + 2T\right)T^{2(s-1)} \tag{14}$$

Taking the logarithm yields:

$$\ln \dot{\xi} \cong \frac{-sE_{eff}}{k_B T} + \ln\left(\frac{E_{eff}}{k_B} + 2T\right) + 2(s-1)\ln T + A_6 \tag{15}$$

Considering again that the variation in lnT is generally much smaller than the variation in $E_{eff}/k_B T$, $\ln \dot{\xi}$ may be plotted versus $-E_{eff}/k_B T$ and s can be obtained from the slope using:

$$k_B \frac{d\ln\dot{\xi}}{d\,1/T} \cong -sE_{eff} - k_B T\left(2(s-1) + \left[\frac{E_{eff}}{2k_B T} + 1\right]^{-1}\right) \tag{16}$$

$$\cong -s(E_{eff} + 2k_B T) - k_B T\left(-2 + \left[\frac{E_{eff}}{2k_B T} + 1\right]^{-1}\right) \tag{17}$$

As in general $y = E_{eff}/k_B T \gg 1$, the second term on the right hand side in the latter equation is much smaller than the first and thus one can obtain the following useful approximation:

$$k_B \frac{d\ln\xi}{d\,1/T} \cong -s\left(E_{eff} + 2k_B T_{av}\right) \approx k_B \frac{d\ln\dot{\xi}}{d\,1/T} \tag{18}$$

However, as indicated by the use of the $\approx$ symbol, the latter approximation in this equation is less accurate than the first. A significantly better approximation of Eq. 17 can be obtained if instead of neglecting both the $E_{eff}\,y^{-1}$ and $E_{eff}\,y^{-2}$ terms, only the $E_{eff}\,y^{-2}$ term is neglected. This leads to:

$$k_B \frac{d\ln\dot{\xi}}{d\,1/T} \cong -s(E_{eff} + 2k_B T_{av}) + 2k_B T_{av} \tag{19}$$

Here we have again neglected the variation in T over the temperature interval and used T_{av}. From the latter equation follows that s can be obtained from the slope of a plot of $\ln\dot{\xi}$ vs. 1/T. In Eq. 19 we may, similar to Eq. 13 and again as a result of the taking of the logarithm, insert any variable proportional to $\dot{\xi}$ in place of $\dot{\xi}$. For DSC this means that we can use the heat flow, q(T), instead of $\dot{\xi}$.

3.3   Determination of activation energies

From Eq. 11 follows that for temperature, T_f, at constant α_{ext} it holds:

$$\ln \frac{\beta}{T_f^2} = -\frac{E_{eff}}{k_B T_f} + C_1 \tag{20}$$

6

C_1 is a constant which depends on the reaction stage. This equation is similar to the one used in the so-called Kissinger method, but the latter is usually obtained via a different set of assumptions (see Ref. [6,23]).

In a previous paper [20] it was shown that the Kissinger analysis is more accurate than the so-called Ozawa method which is derived on the basis of a different approximation. In the same work a new expression for determination of activation energies was derived:

$$\ln \frac{\beta}{T_f^{1.8}} = -A \frac{E_A}{k_B T_f} + C_2 \qquad (21)$$

with

$$A = 1.0070 - 1.2 \ 10^{-5} \ E_A \quad (E_A \text{ in kJ/mol}), \qquad (22)$$

C_2 is a constant which depends on the reaction stage and on the kinetic model. Hence, to obtain the activation energy with this new method the slope of a plot of $\ln(T_f^{1.8}/\beta)$ versus $1/k_B T_f$ should be calculated, whilst A can be evaluated using this slope as a first approximation for E_A. It was shown that the latter method is even more accurate than the Kissinger method [20].

4 Results and discussion

To evaluate the validity of the presented methods for the determination of s, the first stage of the precipitation in various Al-based based alloys is studied using DSC. Three examples of the application of the methods will be given. Firstly, we will study the precipitation in water-quenched Al-6at%Si. Al-Si is a useful model system as it contains only two phases: the Al-rich phase and the Si phase[*], whilst the solubility of Al in the Si phase is negligible [21]. As in water-quenched Al-6at%Si one single mechanism dominates most of the reaction, it is a good model sample to verify the validity of the model. Secondly, we will consider precipitation in Al-6at%Si cooled at 200°C/min for which two mechanisms have been shown to occur [15]. After consideration of this model alloy we will further apply the method to the study of a transformation in a commercial alloy. For this we have selected the 8090 (Al-Li-Cu-Mg-Zr) alloy for which we will study GPB zone formation and we will compare it to GPB-zone formation in Al-Cu-Mg based alloys.

4.1 Quenched Al-6at%Si

A DSC curve of water-quenched (WQ) Al-6at%Si is presented in Fig 1. This figure shows that the entire exothermic effect can be fitted well with the theory presented in Section 3.1 considering two processes. In the first part of the reaction, which will be used below to calculate s with the newly derived methods, only process 1 is important. In Fig. 2 plots of ln q and ln ΔQ(T) vs. 1/T for this DSC experiment are presented. In agreement with the theory in Section 3.2 both plots are straight lines and in accordance with Eq. 18 the slopes of the two lines are about equal. In previous experiments E_{eff} for precipitation in Al-Si was determined as 93.5 kJ/mol (0.97 eV) [14], and thus s can be calculated from the slopes of the plots in

---

[*] However, some authors (24,25,26) have interpreted low temperature resistometric experiments on quenched Al-Si alloys by assuming the existence of precursor phases/states, notably GP zones or Si clusters, but no microstructural evidence of their existence has been reported in literature. Hence, the existence of such precursors is uncertain, and as DSC heat effects due to their formation or dissolution have not been detected in the present work nor in previous work (14,15), heat effects in our DSC and calorimetry experiments on Al-Si alloys are interpreted as reflecting the precipitation and dissolution of the equilibrium phase only.

Fig. 2 by using the appropriate equations in section 3.2. Taking the slope from this data between 5% and 25% of the maximal exothermic heat flow this results in s = 1.50 and s = 1.46, for Eq. 13 and Eq. 19, respectively. These values are consistent with diffusion controlled growth of pre-existing nuclei (s = 1½) and are thus in agreement with earlier results [15]. It is further noted that process 2 as indicated in Fig. 1 starts too late to have an effect on the present analysis.

Having verified that the methods described by Eqs. 13 and 19 yield identical values of s, we will, in the following, limit our attention to the method most easily applied to the experimental data under consideration. Thus, for a derivative method like DSC, Eq. 19 will be used.
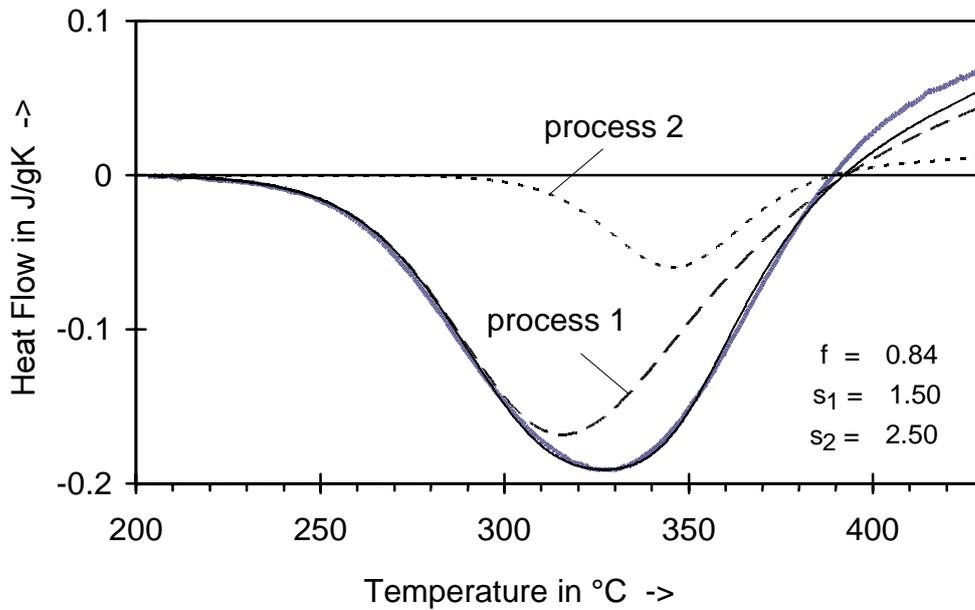
Fig. 1   DSC curve (β = 20°C/min) of water-quenched Al-6Si aged for 1 day at room temperature (thick, grey line). The fit (thinner, black line) is obtained with the model presented in Section 3.1. Also indicated are the contributions of the two processes (dotted lines).

4.2   Al-6at%Si cooled at 200°C/min

It has been shown before that for the Al-6at%Si cooling at 200°C/min after solution treatment is sufficiently fast to suppress precipitation during cooling [15]. The Si precipitation effect during subsequent DSC heating of this supersaturated alloy can be fitted well with the theory presented in Section 3.1, provided two mechanisms, with s equalling 0.5 and 1.5, are taken into account (see Fig. 3). This indicates that precipitation occurs via two mechanisms: growth of coarse, undissolved Si particles (at the solution treatment temperature only 1.3at% Si can dissolve) and growth of pre-existing small nuclei. In the present work we will use the methods introduced in Section 3.2 to directly derive that precipitation starts by growth of undissolved Si particles. First we calculate the effective value of the transformation exponent s in the course of the reaction using Eq. 19. The results presented in Fig. 4 show that s is initially 0.5 and subsequently increases to a value slightly larger than 1 before decreasing. Comparison with the DSC curve shows that the decrease is related to impingement and hence the s values calculated with Eq. 19 for this stage of the reaction are not valid. However, the initial value of 0.5 and the subsequent increase clearly show that i) the first process to occur is growth of undissolved Si particles, and ii) a second process with s > 1 starts shortly after. This is consistent with the fit of the complete curve as given in Fig. 3 and thus confirms that the methods presented in Section 3.2 are sound.
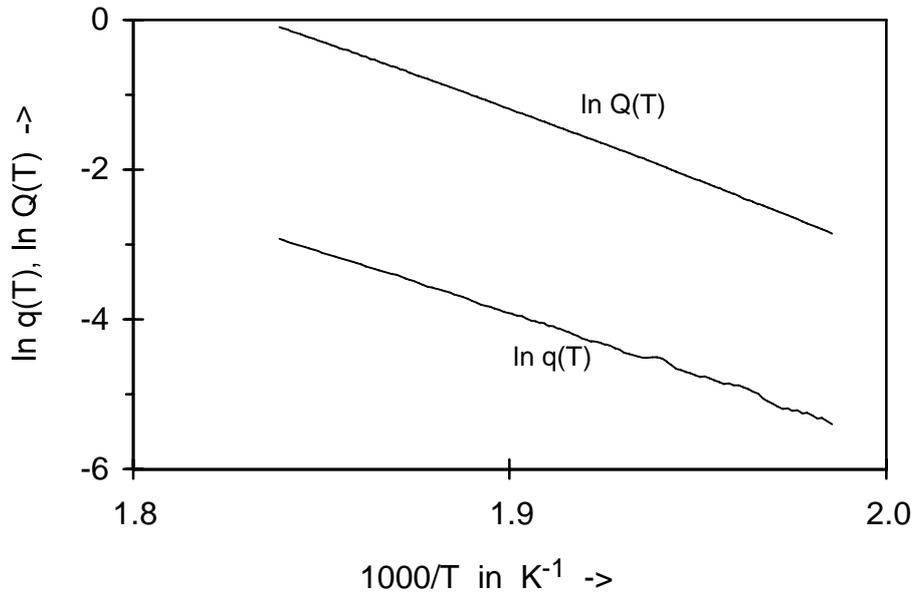
Fig. 2   Logarithm of the total evolved heat and the logarithm of the heat flow measured from DSC vs. 1/T for water quenched Al-6Si. Heating rate is 20°C/min.

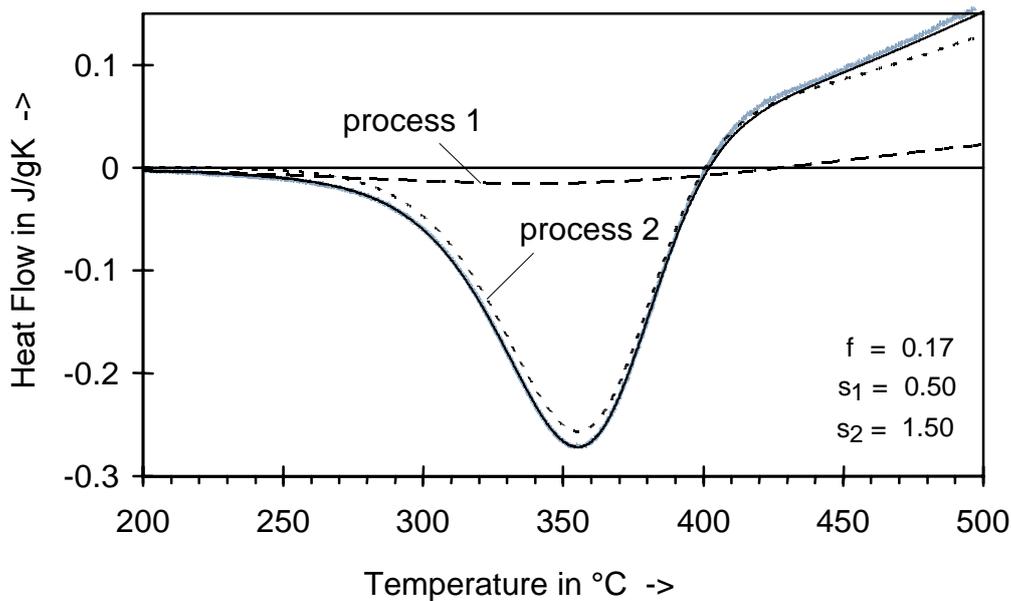Fig. 3   DSC curve ($\beta = 5$°C/min) of Al-6Si cooled at 200°C/min after solution treatment at 550°C (thick, grey line). The fit (thinner, black line) is obtained with the model presented in Section 3.1. Also indicated are the contributions of the two processes (dotted lines).

To obtain a further check of the validity of the interpretations of the precipitation in Al-6at%Si, we performed isothermal calorimetry experiments on the same alloy after solution treatment (2 h at 550°C) and subsequent cooling in a furnace at calorimeter temperature. As cooling to the calorimeter temperature was completed within about 2 minutes, the cooling rate achieved for these specimens is similar to the cooling rate of the specimen used for the DSC curve in Fig. 3 (200°C/min), and both experiments should show similar reaction mechanisms. For isothermal experiments it is expected that nucleation rates are

either constant or zero and it can be derived that for the initial stages of the process, when impingement is negligible, the amount transformed is given by [9]:

$$\xi = A_7 t^{n_1} + A_8 t^{n_2} \qquad (23)$$

where $n = m$ for a process with zero nucleation rate and $n = m + 1$ for a process with constant nucleation rate. Note that provided the assumptions concerning the type of temperature dependence of the nucleation and growth processes (both Arrhenius type) hold, the parameter n in isothermal studies should equal s in non-isothermal studies. If, as obtained from Fig. 4, precipitation is due to growth of coarse, undissolved Si particles and growth of pre-existing small nuclei, $n_1 = 0.5$ and $n_2 = 1.5$. In the limit of t approaching zero, the term with the smallest exponent will be dominant and hence we derive that for this stage the reaction rate is given by:

$$\dot{\xi} = A_7 n_1 t^{n_1 - 1} \qquad (24)$$

And it follows:

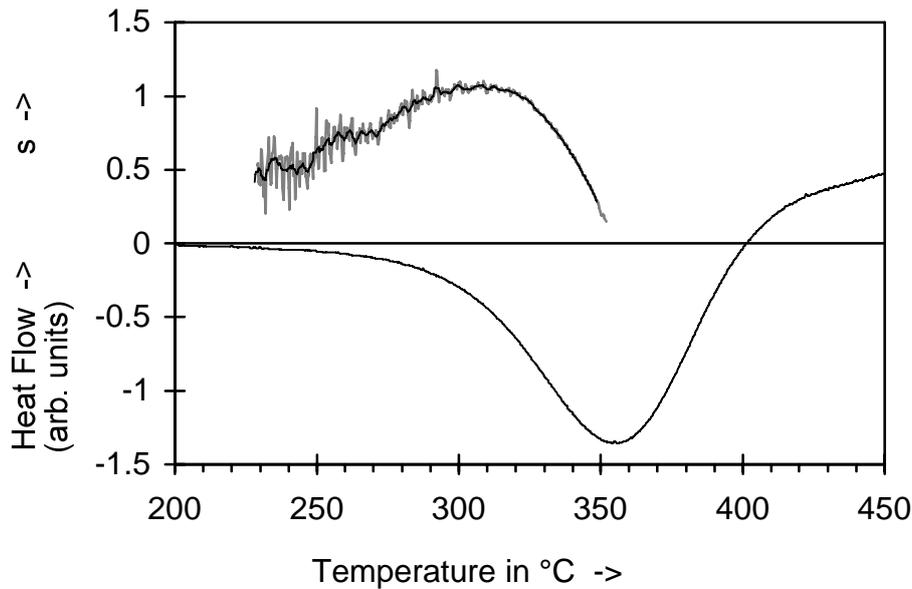$$\frac{d \ln \dot{\xi}}{d \ln t} + 1 = n_1 \qquad (25)$$

Fig. 4   DSC curve of Al-6at%Si cooled at 200°C/min (lower curve). The upper curve is the transformation exponent s derived from the DSC curve using Eq. 19 (darker curve is a smoothed curve). Heating rate is 5°C/min.

Similar to Eqs. 13 and 19, again as a result of the taking of the logarithm and the derivative, any variable proportional to $\dot{\xi}$ can be inserted in place of $\dot{\xi}$. For isothermal calorimetry this means that we can use the heat flow, $q(T)$ (and even the uncalibrated heat flow), instead of $\dot{\xi}$. Using the above equation n was calculated from the isothermal calorimetry curve and the result is reported in Fig. 5. From this figure it is observed that initially n is about 0.5 and increases as the transformation progresses, before decreasing when impingement becomes important. These findings are in line with those made from the DSC experiments using the theory outlined in Section 3.1 and the new analysis methods outlined in Section 3.2. This again indicates that the latter methods are sound.
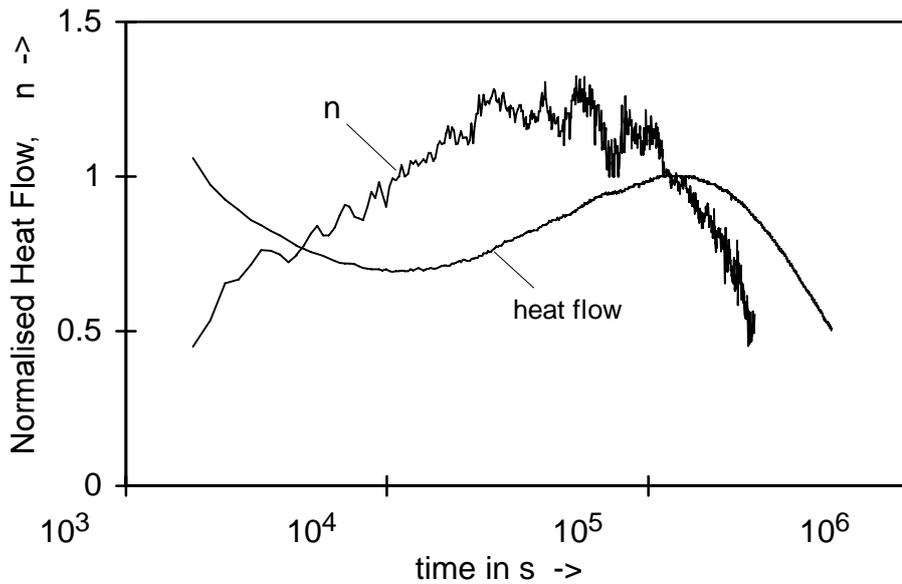
10

Fig. 5   Normalised heat flow from isothermal calorimetry of furnace cooled Al-6at%Si with the n value derived from Eq. 25. Temperature is 190°C.
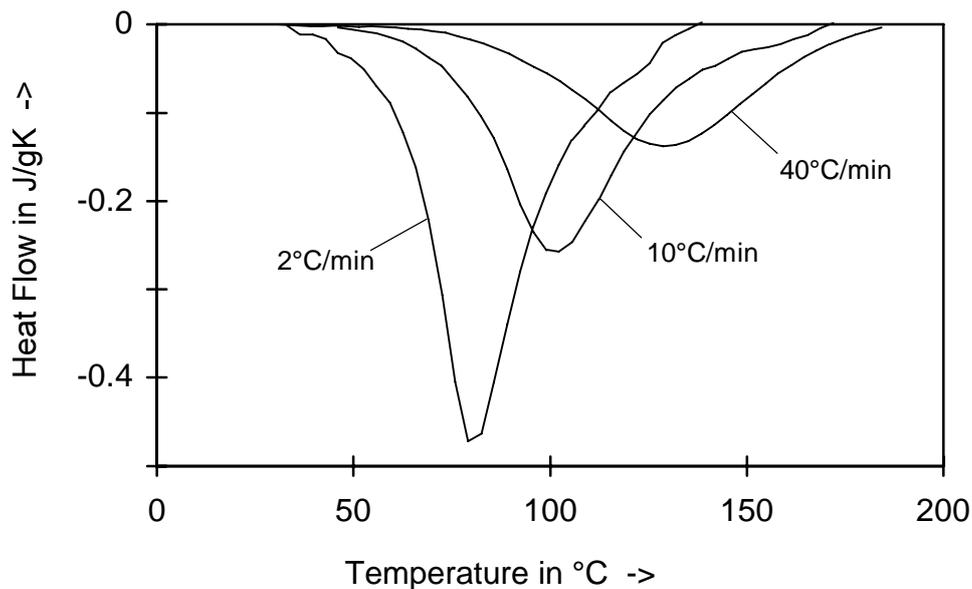

Fig. 6   DSC curves of the water-quenched 8090 (Al-Li-Cu-Mg-Zr) alloy.

4.3   GPB-zone formation in Al-Cu-Mg based alloys

In Al-Cu-Mg based alloys the first stages of precipitation at low temperatures generally involve the formation of GPB zones [27,28]. As a further example of application of the methods for the determination of s we will consider the GPB zone formation effect in an 8090 (Al-Li-Cu-Mg-Zr), an Al-Cu-Mg-Zr and an Al-Cu-Mg alloy.

DSC experiments on the solution treated 8090 alloy were started 5 minutes after quenching, and the heat effects due to GPB-zone formation for various heating rates are presented in Fig. 6. The effective

activation energy for GPB zone formation in the 8090 alloy obtained from these experiments using Eq. 21 equals 67 kJ/mol (0.69 eV) (see also Ref. 29). Subsequently, the transformation exponent s was obtained from the part of the DSC curves at which the heat flow is about 0.1 to 0.35 of the peak value using the two methods outlined above. Also in this case plots of ln q and ln ΔQ(T) vs. 1/T were straight and the resulting s values calculated from the slopes of the plots are presented in Table 2. This table shows that the s values obtained for the different heating rates are consistent, and that both methods yield about the same value for s. This again indicates that the methods derived in Section 3.2 are sound.

The same analysis was performed on DSC curves of water-quenched Al-Cu-Mg and Al-Cu-Mg-Zr alloys. The effective activation energy is taken as 67 kJ/mol [16]. The values of s calculated from the part of the DSC curves at which the heat flow is 0.1 to 0.35 of the peak value are given in Table 3. In the same table also the value of n obtained from an isothermal calorimetry experiment at 30°C on the Al-Cu-Mg-Zr alloy analysed using Eq. 25 is presented. For the other two alloys this analysis could not be performed because: i) the GPB formation in the Al-Cu-Mg alloy occurs too fast to be able to detect the onset of the effect with isothermal calorimetry, and ii) for the powder metallurgical 8090 alloy insufficient material was available to produce calorimetry samples.

In trying to explain the calculated s values it is first noted that for the Al-Cu-Mg-Zr alloy s is close to the theoretical value for a process which combines nucleation and diffusion-controlled growth (s = $2\frac{1}{2}$), and is interpreted accordingly. The isothermal calorimetry experiment on the same alloy confirmed this finding, as n was observed to be 2.5. For Al-Cu-Mg and Al-Cu-Mg-Li-Zr (8090) s values are close to the value for diffusion-controlled growth of small pre-existing nuclei (s = $1\frac{1}{2}$). Hence, it is clear that this is the dominating process for GPB zone formation in these alloys and that nucleation of new zones during the DSC effect is generally limited. In the 8090 alloy s is always somewhat lower than 1.5 and decreases slightly with increasing heating rate. These observations can be explained as follows. Firstly, as the stability of nuclei is temperature dependent, some of the nuclei which start growing right at the beginning of the exothermic DSC effect may become unstable as the temperature increases, and subsequently dissolve. One may, in a sense, consider this as a negative nucleation rate, and in such a case s will decrease as the rate of removal of nuclei increases. If a large number of nuclei is present at the start of a DSC run, s will be 1.5 for low heating rates and, as the rate of removal of nuclei will increase with heating rate, s will decrease with increasing heating rate. This can broadly explain the heating rate dependence of s for the 8090 alloy. Secondly, Table 2 indicates that for the 8090 alloy even at very low heating rates s always remains somewhat below the value of 1.5. As a precipitation process via growth on particles of finite size will have an s value less than 1.5, this may be understood if at the start of the DSC experiment GPB zones have already grown beyond the stage of being mere nuclei. Indeed, earlier findings [29] which indicated that in the 8090 alloys some precipitation had already occurred before the start of the DSC experiment are consistent with this.

In summarising this section we have shown that the methods derived in section 3.2 can be successfully applied to the study of GPB zone formation. The analysis indicates that in Al-Cu-Mg and Al-Li-Cu-Mg-Zr alloys GPB zone formation occurs via growth of pre-existing nuclei, whilst in Al-Cu-Mg-Zr GPB formation occurs via nucleation and growth. A thorough discussion of the differences in transformation between the alloys is beyond the scope of the present paper. It is however noted that i) a Zr / vacancy complex has a high binding energy, and ii) for nucleation of GP zones generally vacancies are required. This may well provide the basis for an explanation for the observed differences in transformation between the alloys, whilst in the 8090 alloy Li / vacancy complexes may further complicate the picture.

Table 2   The transformation exponent s obtained from DSC experiments on an 8090 (Al-Li-Cu-Mg-Zr) alloy.

	2°C/min	10°C/min	40°C/min
Eq. 13 (integral method)	1.4±0.1	1.3±0.1	1.2±0.1
Eq. 19	1.3±0.1	1.2±0.1	1.2±0.1

Table 3   The transformation exponent s obtained from DSC experiments and n obtained from isothermal calorimetry. Heating rate is (about) 20°C/min.

	s	n
Al-Cu-Mg	1.6	-
Al-Cu-Mg-Zr	2.4	2.5
Al-Cu-Mg-Li-Zr	1.3	-

4.4 Recrystallisation of deformed FCC metals

To further study the application of the methods in Section 3.2 we will consider a reaction for which we can expect a constant rate of movement of the interface (linear growth), and thus a relatively high value for s. For this we have selected recrystallisation of deformed FCC metals which have been studied both at constant temperature and during linear heating by Häßner, Schönborn, and co-workers [30,31,32] using a differential heat flux calorimeter. We will first consider recrystallisation in 99.999% Ag plastically deformed in torsion up to a shear strain of 4.8 [30]. In Fig. 7 a plot of ln q vs. 1/T (q(T) is obtained from Fig. 1 in Ref. [30]) up to a fraction transformed of about 10% is presented. In accordance with our model this plot shows a linear relation. Schönborn and Häßner obtained an average activation energy of 80±2 kJ/mol for this early stage of the reaction, whilst for later stages the activation energy increases to reach an average of 84.6kJ/mol. The former value is appropriate for the present analysis of the early stage of the reaction, and from the slope of the line in Fig. 7 in combination with Eq. 19 it is obtained: s = 4.0±0.1. The latter value agrees very well the value expected for a nucleation and growth type reaction with linear growth (s = 4), and is incompatible with growth of pre-existing nuclei, as the Avrami exponent of 3 resulting from Schönborn and Häßner's analysis [30] suggests. This analysis shows that, at least in the first stages of the reaction, recrystallisation occurs via nucleation and growth.

We applied a similar analysis to the first 10% of the heat effect due to recrystallisation of 99.997% Cu cold rolled to a reduction of 80% (see Refs. [31,32]). For linear heating experiments (Fig. 3 in Ref. [31]) we obtained s = 4.7±0.2. For this reaction also an activation energy analysis and isothermal experiments have been presented by Häßner (Fig. 2 in Ref. [31]). Analysing this data with Eq. 25 yields n = 4.6±0.2, and thus s and n are equal within experimental error. The latter demonstrates again that the theory for linear heating presented in Section 3.2 is fully compatible with a classical analysis of isothermal data. The values of n and s for the recrystallisation of Cu (4.6) are higher than the value for nucleation and linear growth (4), and unlike recrystallisation of Ag, an explanation for the values of n and s is not straightforward. Again, a detailed discussion would be beyond the scope of the present paper, which aim is limited to highlighting the application of the methods outlined in Section 3.2. It is suggested that possible explanations include an autocatalytic process (i.e. s − m > 1) or a reaction with accelerated interface movement (i.e. m > 3).

These examples further illustrate the power of the methods presented in section 3.2, which, in addition, only take a fraction of the time necessary to perform the type of analyses suggested by Schönborn and Häßner [30].
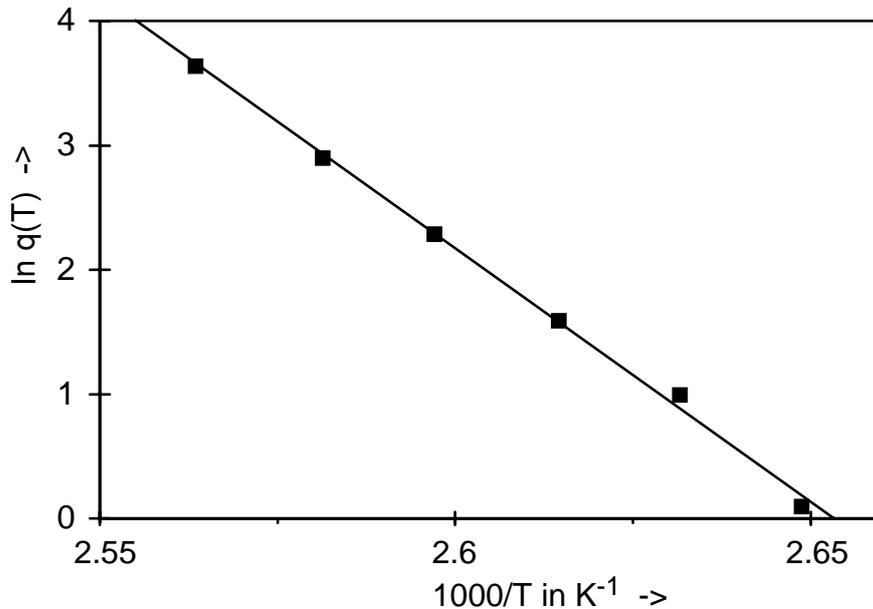
Fig. 7   Plot of the logarithm of the heat flow measured from DSC vs. 1/T for recrystallisation of Ag. (Data from Ref. [30].)

Conclusions

The transformation exponent s which is comparable to the Avrami parameter n in isothermal studies contains information concerning the mechanism of a reaction. Two methods for the determination of s from experiments performed at constant heating rate are derived. The methods consist of plotting the logarithm of the reaction rate or the logarithm of the amount transformed for the first stages of the reaction vs. 1/T, and s can subsequently be calculated from the slope of the straight line. Application to the DSC heat effect of precipitation in quenched Al-6at%Si proves that the methods are consistent and accurate.

As examples of application precipitation in slowly cooled Al-6at%Si, GPB-zone formation in Al-Cu-Mg based alloys, and recrystallisation of deformed FCC metals were analysed. For the slowly cooled Al-6at%Si precipitation of Si starts with a process for which s equals 0.5, indicating growth of undissolved coarse Si particles. It was further shown that in Al-Cu-Mg and Al-Cu-Mg-Li-Zr GPB-zone formation occurs mainly via the growth of pre-existing nuclei (s = 1.5), whilst in Al-Cu-Mg-Zr it occurs via nucleation and growth (s = 2.5). Also recrystallisation of deformed Ag and Cu could be analysed successfully.

Acknowledgements

Notes added after publication

More examples of applications are given in:
M.J. Starink and A.-M. Zahra, Phil. Mag. A, 1998, vol. 77, pp. 187-199

14

M.J. Starink, C.Y. Zahra and A.-M. Zahra, J. Therm. Anal., 1998, vol. 51, pp. 933-942

M.J. Starink, Mater. Sci. Eng. A, 1999, vol. A276, pp. 289-292

M.J. Starink and A.-M. Zahra, Acta Mater., 1998, vol. 46, pp. 3381-3397

M.J. Starink, P. Wang, I. Sinclair and P.J. Gregson, Acta Mater., 1999, vol. 47, 3841-3853.

It is noted that models presented in Refs. 10, 11 have been proven to be incorrect.

References

1 J.W. Christian, The Theory of Transformation in Metals and Alloys, 2nd ed., Part 1 Pergamon Press, Oxford, UK, 1975.
2 F.L. Cumbrera and F. Sanchez-Bajo, Thermochim. Acta 266, (1995) 315.
3 V. Sessa, M. Fanfoni and M. Tomellini, Phys. Rev. B 54, (1996) 836.
4 E. Woldt, J. Phys. Chem. Solids 53, (1992) 521.
5 P. Krüger, J. Phys. Chem. Solids 54, (1993) 1549.
6 J.M. Criado and A. Ortega, Acta Metall. 35, (1987) 1715.
7 Eon-Sik Lee and Young G. Kim, Acta Metall. Mater. 38, (1990) 1677.
8 Eon-Sik Lee and Young G. Kim, Acta Metall. Mater. 38, (1990) 1669.
9 M.J. Starink, J. Mater. Sci. 32, (1997) 4061
10 V. Erukhimovitch and J. Baram, Phys. Rev. B 50, (1994) 5854.
11 V. Erukhimovitch and J. Baram, Phys. Rev. B 51, (1995) 6221.
12 J.B. Austin and R.L. Rickett, Trans. Am. Inst. Min. Engrs. 135, (1939) 396.
13 M.J. Starink and A.-M. Zahra, Mater. Sci. Forum 217-222, (1996) 795.
14 M.J. Starink, J. Mater. Sci. Lett. 15, (1996) 1747.
15 M.J. Starink and A.-M. Zahra, Thermochim. Acta. 292, (1997) 159.
16 A.-M. Zahra, C.Y. Zahra, C. Alfonso and A. Charai, Scr. Mater. 39, (1998) 1553.
17 M.J. Starink and P.J. Gregson, Mater. Sci. Eng. A 211, (1996) 54.
18 M.J. Starink, A.J. Hobson and P.J. Gregson, Scr. Metall. Mater. 34, (1996) 1711.
19 C.Y. Zahra and A.-M. Zahra, Thermochim. Acta 276, (1996) 161.
20 M.J. Starink, Thermochim. Acta 288, (1996) 97.
21 J.L. Murray and A.J. McAlister, Bull. Alloy Phase Diagr. 5, (1984) 74.
22 M. van Rooyen and E.J. Mittemeijer, Metall. Trans. A 20, (1989) 1207.
23 E.J. Mittemeijer, J. Mater. Sci. 27, (1992) 3977.
24 A. Sakakibara and T. Kanadani, Mem. Fac. Eng. Okayama University 24, (1990) 11.
25 H. El Sayed and I. Kovács, Phys. Stat. Sol. A 24, (1994) 123.
26 E. Ozawa and H. Kimura, Mater. Sci. Eng. 8, (1971) 327.
27 S.P. Ringer, K. Hono, I.J. Polmear and T. Sakurai, Appl. Surf. Sci. 94/95, (1996) 253.
28 A.K. Jena, A.K. Gupta and M.C. Chaturvedi, Acta Metall. 37, (1989) 37.
29 M.J. Starink and P.J. Gregson, Scr. Metall. Mater. 33, (1995) 893.
30 K.-H. Schönborn and F. Häßner, Thermochim. Acta 86, (1985) 305.
31 F. Häßner, in R.D. Shull and A. Joshi (eds.), 'Thermal Analysis and Metallurgy', The Mineral, Metals & Materials Society, 1992, p. 233
32 U. Meyer, Ph.D. Thesis, Technische Universität Braunschweig, Germany, 1989